

Neutron star cooling: theoretical aspects and observational constraints

D.G. Yakovlev^{a,*}, O.Y. Gnedin^b, A.D. Kaminker^a, K.P. Levenfish^a, A.Y. Potekhin^a

^a *Ioffe Physical Technical Institute, Politekhicheskaya 26, 194021 St. Petersburg, Russia*

^b *Space Telescope Science Institute, 3700 San Martin Drive, Baltimore, MD 21218, USA*

Received 29 November 2002; received in revised form 7 April 2003; accepted 15 July 2003

Abstract

The cooling theory of isolated neutron stars is reviewed. The main cooling regulators are discussed, first of all, operation of direct Urca process (or similar processes in exotic phases of dense matter) and superfluidity in stellar interiors. The prospects to constrain gross parameters of supranuclear matter in neutron star interiors by confronting cooling theory with observations of isolated neutron stars are outlined. A related problem of thermal states of transiently accreting neutron stars with deep crustal heating of accreted matter is discussed in application to soft X-ray transients.

© 2003 COSPAR. Published by Elsevier Ltd. All rights reserved.

Keywords: Neutron stars; Neutron star cooling; Urca process

1. Introduction

Our knowledge of neutron star (NS) interiors is still uncertain. For instance, the fundamental problem of the equation of state (EOS) at supranuclear densities in NS cores is not solved. Microscopic calculations are model dependent and give a large scatter of possible EOSs (e.g., Lattimer and Prakash, 2001), from stiff to soft ones, with different compositions of inner NS cores (nucleons, pion or kaon condensates, hyperons, quarks). The NS cooling theory enables one to study the internal structure of NSs by confronting the cooling models with observations.

Neutron stars are born hot in supernova explosions, with internal temperature $T \sim 10^{11}$ K, but gradually cool down. In about 30 s after the birth a star becomes transparent for neutrinos generated in its interiors. In the following neutrino-transparent stage the cooling is realized via neutrino emission from the entire stellar

body and via heat transport to the surface resulting in the thermal emission of photons.

The foundation of the strict NS cooling theory was laid by Tsuruta and Cameron (1966). The recent development of the theory has been reviewed, e.g., by Pethick (1992), Page (1998a,b), and Yakovlev et al. (1999). Here, we discuss the current state of the theory as confronted with observations of isolated NSs and outline also a related problem of accreting NSs with application to soft X-ray transients.

2. Cooling calculations and main cooling regulators

The hydrostatic structure of NSs can be regarded as temperature-independent. For a given EOS of dense matter, one can construct a sequence of NS models with different central densities ρ_c , masses M and radii R (M means gravitational mass, and R circumferential radius). For many EOSs, low-mass NSs (with $\rho_c \lesssim 2\rho_0$, where $\rho_0 \approx 2.8 \times 10^{14}$ g cm⁻³ is the density of saturated nuclear matter) contain the nucleon cores (neutrons, n, with an admixture of protons, p, electrons, e, and possibly muons). Massive NSs have the inner cores whose

*Corresponding author. Tel.: +7-812-247-9180; fax: +7-812-550-4890.

E-mail address: yak@astro.ioffe.ru (D.G. Yakovlev).

composition is very model dependent (e.g., Lattimer and Prakash, 2001).

NS cooling is governed by general relativistic equations (Thorne, 1977) of heat diffusion inside the star. Their solution gives the distribution of the temperature T inside the star versus time t , and the effective surface temperature $T_s(t)$. The main ingredients of the cooling theory are the neutrino emissivity Q , heat capacity C and thermal conductivity of NS matter.

It is conventional (Gudmundsson et al., 1983) to divide the NS into the interior and the outer heat-blanketing envelope which extends to the density $\rho_b \sim (10^{10} - 10^{11}) \text{ g cm}^{-3}$ ($\sim 100 \text{ m}$ under the surface). The thermal structure of the envelope is studied separately in the stationary, plane-parallel approximation to relate T_s to the temperature T_b at $\rho = \rho_b$. The diffusion equations are solved then at $\rho \geq \rho_b$.

The NS thermal luminosity is $L_\gamma = 4\pi\sigma R^2 T_s^4(t)$. Both, L_γ and T_s , refer to a locally-flat reference frame on the NS surface. A distant observer would register the “apparent” luminosity $L_\gamma^\infty = L_\gamma(1 - r_g/R)$ and the “apparent” effective temperature $T_s^\infty = T_s\sqrt{1 - r_g/R}$, where $r_g = 2GM/c^2$ is the Schwarzschild radius. If the surface temperature is nonuniform (e.g., in the presence of a strong magnetic field), L_γ^∞ is determined by a properly averaged surface temperature (e.g., Potekhin and Yakovlev, 2001).

The theory provides *cooling curves*, $T_s^\infty(t)$, to be compared with observations. One can distinguish three cooling stages: the internal relaxation stage ($t \lesssim 10\text{--}50$ years; Lattimer et al., 1994; Gnedin et al., 2001), the neutrino cooling stage (the neutrino luminosity $L_\nu \gg L_\gamma$, $t \lesssim 10^5$ years), and the photon stage ($L_\nu \ll L_\gamma$, $t \gtrsim 10^5$ years). After the thermal relaxation, the redshifted temperature $\tilde{T}(t) = T(r, t)e^{\Phi(r)}$ becomes constant throughout the stellar interior ($\Phi(r)$ being the metric function which determines gravitational redshift), and the problem reduces to solving the global thermal-balance equation,

$$\begin{aligned} C_{\text{tot}}(\tilde{T}) \frac{d\tilde{T}}{dt} &= -L_\nu^\infty(\tilde{T}) - L_\gamma^\infty(T_s), \\ L_\nu^\infty(\tilde{T}) &= \int dV Q(T) e^{2\Phi}, \\ C_{\text{tot}}(\tilde{T}) &= \int dV C(T), \end{aligned} \quad (1)$$

where dV is a proper volume element, C_{tot} is the total NS heat capacity, and L_ν^∞ is the neutrino luminosity as detected by a distant observer.

The main cooling regulators at the neutrino cooling stage are: (1) neutrino emission in NS interiors, and (2) the effects of baryon superfluidity on this emission.

1. The major neutrino mechanisms in nucleon matter at $\rho \lesssim 2\rho_0$ are modified Urca (Murca) process and NN-bremsstrahlung (brems); see Table 1, where N is a nucleon, n or p. These mechanisms are relatively weak and produce *slow* cooling. At higher ρ , the neutrino emission can be strongly enhanced by the onset of direct Urca (Durca) process (Lattimer et al., 1991) in nucleon matter or similar (but somewhat weaker) processes in exotic phases of matter. These processes (Table 2, where q is a quasiparticle, while u and d are quarks) can enhance the neutrino emissivity by 2–7 orders of magnitude and lead to *fast* cooling. An example, the enhancement by Durca process, is shown on the right panel of Fig. 1 and discussed in the next section. In nonsuperfluid matter, the emissivities of slow and fast neutrino processes can be written as

$$Q_{\text{slow}} = Q_s T_9^8, \quad Q_{\text{fast}} = Q_f T_9^6, \quad (2)$$

where $T_9 = T/(10^9 \text{ K})$, while Q_s and Q_f are slowly varying functions of ρ (Tables 1 and 2).

2. It is widely accepted that dense matter can be superfluid (e.g., Lombardo and Schulze, 2001; also see Yakovlev et al., 2001a, for references). Microscopic calculations predict superfluidity of neutrons in NS crusts and cores, and superfluidity of protons in NS cores; they predict also superfluidity of hyperons or quarks. A superfluidity of any baryon species is characterized by its own density dependent critical temperature $T_c(\rho)$ which is very model dependent and ranges from $\sim 10^8$ to $\sim 10^{10}$ K. An exclusion is provided by pairing of unlike quarks where T_c can be as high as $\sim 5 \times 10^{11}$ K. Any superfluidity of baryons reduces neutrino processes involving these baryons due to an energy gap in the baryon dispersion relation. When T falls below T_c , the superfluidity initiates also a specific neutrino emission due to Cooper pairing of baryons (Flowers et al., 1976). In addition, it affects baryon heat capacity (e.g., Yakovlev et al., 1999), but at the neutrino cooling stage this effect is less important than the effect on neutrino emission.

Furthermore, NS cooling can be affected by the thermal conductivity in heat-blanketing envelopes which regulates the relation between T_s and T_b . The conductivity is modified by the presence of light (accreted) elements (Potekhin et al., 1997) or by strong surface magnetic fields (e.g., Potekhin and Yakovlev, 2001;

Table 1

Main processes of slow neutrino emission in nucleon matter: Murca and bremsstrahlung

Process			Q_s (erg cm ⁻³ s ⁻¹)
Murca	$n + N \rightarrow p + N + e + \bar{\nu}$	$p + N + e \rightarrow n + N + \nu$	$10^{20}\text{--}3 \times 10^{21}$
Bremsstrahlung	$N + N \rightarrow N + N + \nu + \bar{\nu}$		$10^{19}\text{--}10^{20}$

Table 2

Leading processes of fast neutrino emission in nucleon matter and three models of exotic matter

Model	Process		Q_f (erg cm ⁻³ s ⁻¹)
Nucleon matter	$n \rightarrow p + e + \bar{\nu}$	$p + e \rightarrow n + \nu$	$10^{26} - 10^{27}$
Pion condensate	$q \rightarrow q + e + \bar{\nu}$	$q + e \rightarrow q + \nu$	$10^{23} - 10^{26}$
Kaon condensate	$q \rightarrow q + e + \bar{\nu}$	$q + e \rightarrow q + \nu$	$10^{23} - 10^{24}$
Quark matter	$d \rightarrow u + e + \bar{\nu}$	$u + e \rightarrow d + \nu$	$10^{23} - 10^{24}$

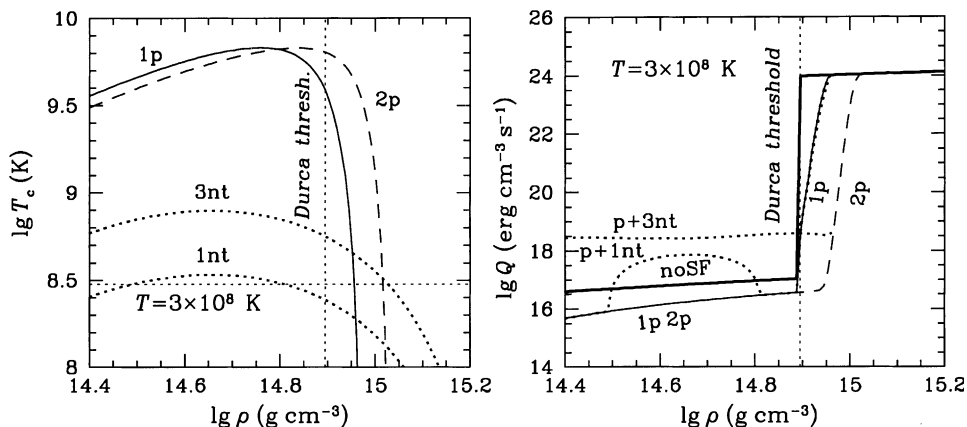


Fig. 1. Left panel: density dependence of the critical temperatures of superfluidity of protons (models 1p and 2p) and neutrons (model 1nt and 3nt) in a NS core; vertical dotted line is the Durca threshold; horizontal line is the temperature $T = 3 \times 10^8$ K adopted on the right panel. Right panel: density dependence of the neutrino emissivity through the NS core at the given T for nonsuperfluid matter (thick solid line), for proton superfluidity 1p or 2p (thin solid or dashed lines), or with added neutron superfluidity 1nt or 3nt (dots).

Yakovlev et al., 2002a, and references therein). These effects are weaker than those cited above. The NS cooling may also be regulated by other factors, particularly, by reheating mechanisms which may operate in NS interiors, for instance, due to frictional dissipation of differential rotation or ohmic decay of magnetic fields. Some of these mechanisms have been reviewed by Page (1998a,b).

3. Observations

We will confront the cooling theory with observations of thermal emission from nine middle-aged isolated NSs. Recently the observations have been reviewed by Pavlov et al. (2002b). The data are summarized in Table 3 and displayed in Figs. 2 and 3. Two young objects (RX

J0822-43, 1E 1207-52) are radio-quiet NSs in supernova remnants; RX J1856-3754 is also a radio-quiet NS. The other objects, Crab, RX J0205+6449, Vela, PSR 0656+14, Geminga, and PSR 1055-52, are observed as radio pulsars. RX J0205+6449 and the Crab pulsar are associated with historical supernovae and their ages are certain. For RX J0822-43, we take the estimated age $t = 2-5$ kyear of the associated supernova (as can be deduced, e.g., from a discussion in Arendt et al., 1991) centered at $t = 3.7$ kyear (Winkler et al., 1988). For 1E 1207-52, we adopt the range from the standard age of the associated supernova (~ 7 kyears) to the four times longer age taking into account slow spindown of NS rotation detected in X-rays (Pavlov et al., 2002a). For Vela, we take the age interval from the standard spindown age to the age reported by Lyne et al. (1996). The

Table 3

Observational limits on surface temperatures of isolated neutron stars

Source	t (kyear)	T_s^∞ (MK)	Confid. (%)	References
PSR J0205+6449	0.82	<1.1	–	Slane et al. (2002)
PSR B0531+21 (Crab)	1	<2.1	–	Tennant et al. (2001)
RX J0822-4300	2–5	1.6–1.9	90	Zavlin et al. (1999)
1E 1207-52	≥ 7	1.1–1.5	90	Zavlin et al. (1998)
PSR 0833-45 (Vela)	11–25	0.65–0.71	68	Pavlov et al. (2001)
PSR B0656+14	~ 110	0.91 ± 0.05	90	Possenti et al. (1996)
PSR 0633+1748 (Geminga)	~ 340	$0.56 (+0.07, -0.09)$	90	Halpern and Wang (1997)
RX J1856-3754	~ 500	0.52 ± 0.07	–	Pons et al. (2002)
PSR 1055-52	~ 530	$0.82 (+0.06, -0.08)$	90	Pavlov and Teter (2002)

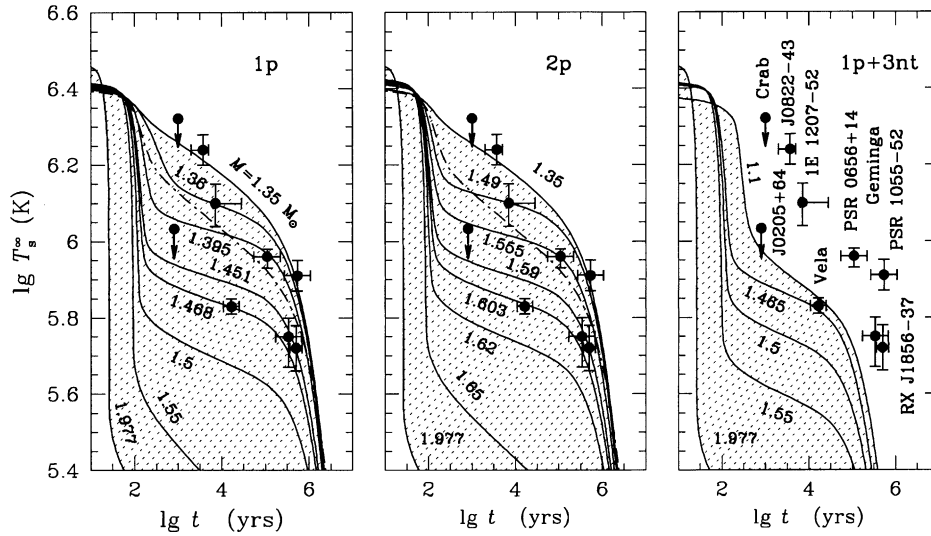


Fig. 2. Observational data on nine NSs compared with the cooling curves of NSs of several masses M for three superfluid models in the NS cores (left panel: 1p; middle panel: 2p; right panel: 1p+3nt). Dot-and-dashed line: cooling of a nonsuperfluid $1.35 M_{\odot}$ NS. Shaded regions are allowed by the assumed models.

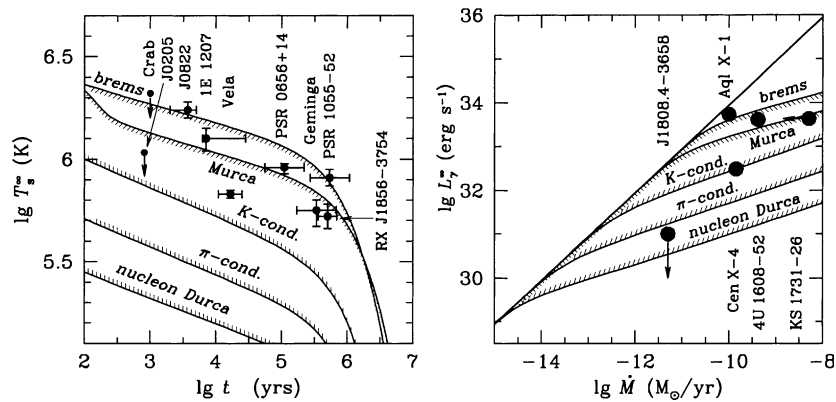


Fig. 3. Observational data confronted with theoretical curves. Left panel: slow cooling of low-mass NSs and rapid cooling of high-mass NSs (with nucleon or exotic inner cores). Right panel: heating curves of low-mass and high-mass accreting NSs compared with observations of several SXRts in quiescence. See text for details.

age of RX J1856-3754 has been revised recently by Walter and Lattimer (2002) from the kinematical reasons; the errorbar is chosen in such a way to clearly distinguish the revised value from the previous one. The ages of other NSs are the standard spindown ages with an uncertainty by a factor of two.

For two youngest sources, RX J0205+6449 and the Crab pulsar, no thermal emission has been detected, but the upper limits on T_s^{∞} have been established. For the next three sources, the values of T_s^{∞} are obtained from the observed X-ray spectra using hydrogen atmosphere models. Such models are more consistent with other information on these sources (e.g., Pavlov et al., 2002b) than the blackbody model of NS emission. On the contrary, for PSR 0656+14, Geminga and PSR 1055-52, we present the values of T_s^{∞} inferred using the blackbody spectrum which is more consistent for these

sources. Finally, for RX J1856-3754 we adopt the values inferred using the analytic fit with Si-ash atmosphere model of Pons et al. (2002).

4. Cooling of neutron stars with nucleon cores

We start with the simplest composition of the NS cores (n, p, and e). Illustrative cooling curves are calculated with our fully relativistic nonisothermal cooling code (Gnedin et al., 2001). In the NS cores, we use a stiff phenomenological EOS proposed by Prakash et al. (1988) (their model I with the compression modulus of saturated nuclear matter $K = 240$ MeV). The maximum-mass configuration has $M = 1.977 M_{\odot}$, $R = 10.754$ km, and $\rho_c = 2.575 \times 10^{15}$ g cm $^{-3}$. The Durca process is open at $\rho \geq \rho_D = 7.851 \times 10^{14}$ g cm $^{-3}$. The NS

model with $\rho_c = \rho_D$ has $M = M_D = 1.358M_\odot$ and $R = 12.98$ km.

The code includes the effects of nucleon superfluidities of three types: singlet-state (1S_0) pairing of free neutrons in the inner crust (with the critical temperature $T_c = T_{\text{cns}}(\rho)$); 1S_0 proton pairing in the core ($T_c = T_{\text{cp}}(\rho)$); and triplet-state (3P_2) neutron pairing in the core ($T_c = T_{\text{cnt}}(\rho)$). The $T_c(\rho)$ dependence has been parameterized by simple equations (e.g., Yakovlev et al., 2002a,b); the adopted models of $T_c(\rho)$ do not contradict numerous microscopic calculations (e.g., Lombardo and Schulze, 2001).

4.1. Nonsuperfluid stellar models

For nonsuperfluid NSs, we have *two* well-known cooling regimes, *slow* and *fast* cooling. The slow cooling takes place in low-mass NSs ($M < M_D$) via neutrino emission produced mainly by Murca process. The cooling curves appear to be almost the same for all M from about $1.1 M_\odot$ to M_D (e.g., Page and Applegate, 1992) being insensitive to EOS (like the dot-and-dashed line in Fig. 2 which can be called *the standard basic cooling curve*). These models of Murca-emitting nonsuperfluid NSs cannot explain the observations of some sources, first of all, PSR J0205+6449 and Vela (too cold), as well as RX J0822-43 and PSR 1055-52 (too hot). The data seem to require both, slower and faster cooling.

The fast cooling occurs via a powerful Durca process at $M > M_D$. The cooling curves are again not too sensitive to the mass and EOS. These NSs are much colder than the slowly cooling ones. The transition from the slow to fast cooling takes place in a very narrow range of M because of the huge difference in the emissivities of Murca and Durca processes, and a sharp threshold of Durca process (right panel of Fig. 1). On the $T_s^\infty - t$ diagram some sources (first of all, Vela, Geminga, RX J1856-3754) fall exactly in this transition zone, and therefore could be explained if they had almost the same mass. This unlikely assumption can be avoided by including the effects of nucleon superfluidity.

4.2. Proton superfluidity and three types of cooling neutron stars

The observations can be explained by cooling of superfluid NSs assuming that the *proton superfluidity is rather strong* at $\rho \lesssim \rho_D$, while the *3P_2 neutron superfluidity is rather weak*. We start with the effects of proton superfluidity neglecting neutron pairing. We take two typical models of proton superfluidity, 1p and 2p, displayed on the left panel of Fig. 1. The appropriate neutrino emissivity over the NS core at $T = 3 \times 10^8$ K is shown on the right panel. The effects of proton superfluidity are seen to be twofold. First, the superfluidity

reduces the neutrino emission in the outer NS core by strongly suppressing Murca or even Durca process at not too high ρ . Second, the proton superfluidity gradually dies out with increasing ρ and removes the reduction of fast neutrino emission. This *broadens* the threshold of fast neutrino emission, creating a *finite transition zone* (which will be denoted as $\rho_s \lesssim \rho \lesssim \rho_f$) between slowly ($\rho \lesssim \rho_s$) and rapidly ($\rho \gtrsim \rho_f$) neutrino emitting layers. Superfluid 2p extends deeper to the NS core and shifts the transition zone to higher ρ . The cooling curves of NSs of different masses with proton superfluidities 1p and 2p are plotted on the left and middle panels of Fig. 2, respectively. We see that the proton superfluidity leads to the *three* representative types of cooling NSs.

Low-mass NSs, where $\rho_c < \rho_s$, have weaker neutrino emission than low-mass nonsuperfluid NSs; they form a class of *very slowly cooling* NSs. Their cooling curves are almost independent of NS mass, proton superfluid model, and EOS in the NS cores. These cooling curves go higher than the basic standard cooling curve, explaining now the observations of RX J0822-43 and PSR 1055-52. Thus we can treat these two NSs as low-mass NSs.

High-mass, rapidly cooling NSs, where $\rho_c \gtrsim \rho_f$, cool mainly via fast neutrino emission from the inner core. The cooling curves are again almost independent of M , EOS and proton superfluidity, and are actually the same as for high-mass nonsuperfluid NSs. All the observed NSs are much warmer than these ones.

Medium-mass NSs ($\rho_s \lesssim \rho_c \lesssim \rho_f$) show cooling which is *intermediate* between very slow and fast; it depends on M , EOS and proton superfluidity. Roughly, the masses of these NSs range from M_D to $1.55 M_\odot$ for 1p superfluid and from 1.4 to $1.65 M_\odot$ for 2p superfluid. By varying ρ_c from ρ_s to ρ_f we obtain a family of cooling curves which fill the space between the curves of low-mass and high-mass NSs. We can select those curves which explain the observations and attribute thus certain masses to the sources (“weigh” NSs, Kaminker et al., 2001). This weighing depends on EOS and proton superfluid model (left and mid panels of Fig. 2). We treat 1E 1207-52, Vela, PSR 0656+14, Geminga, and RX J1856-3754 as medium-mass NSs.

4.3. Mild neutron pairing in the core contradicts observations

Now we switch on 3P_2 neutron pairing in the NS core. Microscopic theories predict this pairing to be weaker than the proton one, with $T_{\text{cnt}}(\rho) \lesssim 10^9$ K. Two models (1nt and 3nt) are presented on the left panel of Fig. 1, with maximum $T_{\text{cnt}}^{\text{max}} \approx 3.4 \times 10^8$ and 8×10^8 K, respectively. The onset of such superfluidity induces a strong neutrino emission due to Cooper pairing of neutrons as shown by dotted lines on the right panel of

Fig. 1. The emissivity in the outer NS core becomes higher than in a nonsuperfluid star and accelerates the cooling. The cooling curves for NSs with 1p proton and 3n neutron superfluids are shown on the right panel of Fig. 2. These NS models cool too fast and contradict observations of many sources. We have checked that any *mild* neutron superfluidity in the core with realistic $T_{\text{cnt}}(\rho)$ profiles and $T_{\text{cnt}}^{\text{max}} \sim (2 \times 10^8 - 2 \times 10^9)$ K contradicts observations of at least some hotter and older objects (independently of the proton pairing) and should be rejected on these grounds. A neutron superfluidity with smaller $T_{\text{cnt}}^{\text{max}}$ appears at late stages of NS evolution and has no effect on cooling of middle-aged NSs.

4.4. Very slowly cooling neutron stars and the physics of the crust

As discussed above, the cooling of low-mass NSs is rather robust against uncertainties of the physics in the NS cores. Their neutrino luminosity is exceptionally low. Accordingly, their cooling is *especially sensitive to the physics of the NS crust*. The cooling of these NSs (contrary to other ones) is strongly regulated by the effects of singlet-state neutron superfluidity in the inner NS crusts, surface magnetic fields and accreted envelopes as described by Yakovlev et al. (2001b, 2002a) and Kaminker et al. (2002). By tuning such factors one can refine the interpretation of the observations of RX J0822-43 and PSR 1055-52.

5. Cooling of neutron stars with exotic cores

At the next step we explore a hypothesis of exotic NS cores adopting the model of neutrino emission given by Eq. (2). Quite generally, we assume the presence of the outer NS core with slow neutrino emission, the inner core with fast neutrino emission, and the intermediate zone ($\rho_s \lesssim \rho \lesssim \rho_f$). Then we obtain three types of cooling NSs similar to those discussed in the previous section: low-mass NSs ($\rho_c \lesssim \rho_s$) which show slow cooling; high-mass NSs ($\rho_c \gtrsim \rho_s$) which show fast cooling via enhanced neutrino emission from the inner cores; medium-mass NSs ($\rho_s \lesssim \rho_c \lesssim \rho_f$) with intermediate cooling.

Left panel of Fig. 3 displays the cooling curves of low-mass and high-mass NSs for several EOSs of NS cores. The EOSs affect the neutrino emission in the inner and outer cores. The real EOS, which *should be the same for all NSs*, is currently unknown.

The outer NS cores are thought to consist of nucleon matter. We present two types of cooling curves of low-mass ($1.3M_\odot$) NSs from the previous section. The *Murca* curve is the standard basic cooling curve. The *brems* curve refers to the very slow cooling inspired by strong proton superfluidity. These are the *upper* cooling

curves for NSs with nonsuperfluid and superfluid outer cores. The cooling curves of medium-mass NSs are lower (as shown by shading).

We present also three cooling curves for high-mass ($\approx 2M_\odot$) NSs. They are calculated (Yakovlev and Haensel, 2003) using a simplified toy model of cooling NSs with three constant rates of fast neutrino emission, Eq. (2), in the inner cores: $Q_f = 10^{27}, 10^{25}$, and 10^{23} erg $\text{s}^{-1} \text{cm}^{-3}$. These rates are appropriate (Table 2) to three EOSs in the inner cores: nucleon matter with open Durca process (curve *nucleon Durca*; will be about the same in the presence of hyperons), pion-condensed matter (*π -cond*), and kaon-condensed (or quark) matter (*K-cond*). They are three possible *lowest* cooling curves. The cooling curves of medium-mass NSs are higher (as shown by shading). For any EOS in NS cores, we have a highest cooling curve of low-mass NSs, a lowest cooling curve of high-mass NSs, and a sequence of cooling curves of medium-mass NSs between the highest and lowest ones. All in all, we present the allowable values of T_s for six different EOSs.

As discussed in Section 4.2, curve *brems* is in better agreement with the observations than *Murca*, for low-mass NSs. All three EOSs in the inner NS cores (*nucleon Durca*, *π -cond*, *K-cond*) do not contradict observations (as concluded by a number of authors, e.g., by Page, 1998a,b). Evidently, it would be most interesting to discover colder NSs to constrain these EOSs.

A rather uniform scatter of the observational points suggests the existence of the representative class of medium-mass NSs. Their mass range is sensitive to the position and width of the transition layer between the slow and fast neutrino emission zones. Unfortunately, these parameters cannot be strongly constrained (Yakovlev and Haensel, 2003) from the current data.

6. Thermal states of transiently accreting neutron stars

Now we discuss the thermal states of accreting NSs in soft X-ray transients (SXRTs). SXRTs undergo (e.g., Chen et al., 1997) the periods of outburst activity (days–months) superimposed with quiescent periods (months–decades). Their activity is most probably regulated by accretion from disks around the NSs. In quiescence, the accretion is switched off or suppressed. Nevertheless, some sources show rather intense thermal radiation indicating that NSs are sufficiently warm. It is quite possible (Brown et al., 1998) that these NSs are warmed up by deep crustal heating (Haensel and Zdunik, 1990) produced by nuclear transformations in the accreted matter while this matter sinks into the inner NS crust (to densities $\rho \gtrsim 10^{11}$ g cm^{-3}) under the weight of newly accreted material. The total energy release is about 1.45 MeV per accreting baryon, and the total heating power is $L_{\text{dh}} \approx 8.74 \times 10^{33} \dot{M} / (10^{-10} M_\odot \text{ yr}^{-1})$ erg s^{-1} , where \dot{M}

is the mass accretion rate. The heat is spread over the NS by the thermal conductivity and radiated away by surface photon emission and neutrino emission from the NS interior. Generally, the surface temperature depends on the NS internal structure.

Neutron stars in SXRTs are thermally inertial objects with the thermal relaxation times $\sim 10^4$ years (Colpi et al., 2001). Their thermal states do not ‘feel’ transient variations of the accretion rate. Thus a thermal state can be determined in the steady-state approximation by solving the thermal balance equation: $L_{\text{dh}}(\dot{M}) = L_{\gamma}^{\infty}(\tilde{T}) + L_{\gamma}^{\infty}$ (cf. Eq. (1)), where $\dot{M} \equiv \langle \dot{M} \rangle$ means the time-averaged accretion rate. A solution gives a *heating curve*, $L_{\gamma}^{\infty}(\dot{M})$, or, equivalently, $T_{\text{s}}^{\infty}(\dot{M})$. The heating curves of accreting NSs are closely related to the cooling curves of isolated NSs (e.g., Colpi et al., 2001; Yakovlev et al., 2003).

On the right panel of Fig. 3, we present the limiting heating curves calculated (Yakovlev et al., 2003) using the toy model of NS thermal structure (Yakovlev and Haensel, 2003). They are analogous to the limiting cooling curves on the left panel. Two upper curves (*brems* and *Murca*) are the heating curves of low-mass $1.16 M_{\odot}$ NSs ($\dot{Q}_{\text{s}} = 3 \times 10^{19}$ and 10^{21} erg $\text{cm}^{-3} \text{s}^{-1}$ in Table 1, respectively). Three lower curves *nucleon Durca*, *π -cond* and *K-cond* are the heating curves of $2 M_{\odot}$ NSs. For any EOS of NS interiors, we have its own upper heating curve and the lower one, and a family of heating curves of medium-mass NSs which fill the space between the upper and lower curves.

These results are confronted with observations of five SXRTs. The data are the same as taken by Yakovlev et al. (2003). We treat L_{γ}^{∞} as the thermal surface luminosity of SXRTs in quiescence, and take the values of L_{γ}^{∞} for Aql X-1, Cen X-4, 4U 1608-522, KS 1731-26, and SAX 1808.4-3658 from Rutledge et al. (2002, 2000, 1999), Wijnands et al. (2002), and Campana et al. (2002), respectively. The value of \dot{M} for KS 1731-26 is most probably an upper limit. No quiescent thermal emission has been detected from SAX J1808.4-3658, and we present the established upper limit of L_{γ}^{∞} . Since the data are rather uncertain we plot the observational points as thick dots.

As seen from Fig. 3, we can treat NSs in 4U 1608-52 and Aql X-1 as low-mass NSs with superfluid cores. NSs in Cen X-4 and SAX J1808.4-3658 seem to require the enhanced neutrino emission and are thus more massive. The status of NS in KS 1731-26 is less certain because of poorly determined \dot{M} ; it may also require enhanced neutrino emission. Similar conclusions have been made by a number of authors (cited in Yakovlev et al., 2003) with respect to some of these sources.

Let us disregard the SAX source for a moment. The observational point for Cen X-4 lies above (or near) all three limiting heating curves for massive NSs. Thus we can treat the NS in Cen X-4 either as high-mass NS

(with kaon-condensed or quark core) or as medium-mass NS (with pion-condensed, or nucleon Durca core). If further observations confirm the current status of SAX J1808.4-3658, then we will have the only choice to treat this NS as a high-mass NS with the nucleon core (and the NS in Cen X-4 as medium-mass NS with the nucleon core). This would disfavor the hypothesis on exotic phases of matter in NS cores.

7. Conclusions

The theory of NS cooling is very flexible and provides many successful cooling scenarios. If thermal states of NSs in SXRTs are determined by deep crustal heating, the theory and observations of isolated NSs and SXRTs can be analyzed together.

Disregarding the observations of SAX J1808.4-3658, the data on isolated NSs and SXRTs imply that: (a) an enhanced neutrino emission operates in massive NSs but its nature is unknown (nucleon Durca, pion- or kaon-condensates, quarks?); (b) representative class of medium-mass NSs is available; (c) the position and width of the transition layer between slowly and rapidly cooling layers in the NS cores are uncertain. If the observations of SAX J1808.4-3658 are relevant to the present analysis, they are in favor of nucleon models of dense matter with open Durca, and they disfavor the models of exotic matter.

Some physical models of NS interiors contradict observations, e.g., the existence of mild ${}^3\text{P}_2$ neutron superfluidity with the maximum $T_{\text{cn}}(\rho)$ in the range from 2×10^8 to 2×10^9 K.

A search for new very cold and very hot NSs would be useful. Very cold NSs would disfavor the models of exotic matter.

Acknowledgements

We are indebted to George Pavlov for providing the data on PSR 1055-52. The work was partly supported by RFBR (Grants No. 02-02-17668 and 03-07-90200).

References

- Arendt, R.G., Dwek, E., Petre, R. An infrared analysis of Puppis A. *Astrophys. J.* 368, 474–485, 1991.
- Brown, E.F., Bildsten, L., Rutledge, R.E. Crustal heating and quiescent emission from transiently accreting neutron stars. *Astrophys. J.* 504, L95–L98, 1998.
- Campana, S., Stella, L., Gastaldello, F., et al. An XMM-Newton study of the 401 Hz accreting pulsar SAX J1808.4-3658 in quiescence. *Astrophys. J.* 575, L15–L19, 2002.
- Chen, W., Shrader, C.R., Livio, M. The properties of X-ray and optical light curves of X-ray novae. *Astrophys. J.* 491, 312–338, 1997.
- Colpi, M., Geppert, U., Page, D., et al. Charting the temperature of the hot neutron star in a soft X-ray transient. *Astrophys. J.* 548, L175–L178, 2001.

- Flowers, E.G., Ruderman, M., Sutherland, P.G. Neutrino-pair emission from finite-temperature neutron superfluid and the cooling of young neutron stars. *Astrophys. J.* 205, 541–544, 1976.
- Gnedin, O.Y., Yakovlev, D.G., Potekhin, A.Y. Thermal relaxation in young neutron stars. *Mon. Not. Roy. Astron. Soc.* 324, 725–736, 2001.
- Gudmundsson, E.H., Pethick, C.J., Epstein, R.I. Structure of neutron star envelopes. *Astrophys. J.* 272, 286–300, 1983.
- Haensel, P., Zdunik, J.L. Non-equilibrium processes in the crust of an accreting neutron star. *Astron. Astrophys.* 227, 431–436, 1990.
- Halpern, J.P., Wang, F.Y.-H. A broadband X-ray study of the Geminga pulsar. *Astrophys. J.* 477, 905–915, 1997.
- Kaminker, A.D., Haensel, P., Yakovlev, D.G. Nucleon superfluidity vs. observations of cooling neutron stars. *Astron. Astrophys.* 373, L17–L20, 2001.
- Kaminker, A.D., Yakovlev, D.G., Gnedin, O.Y. Three types of cooling superfluid neutron stars: theory and observations. *Astron. Astrophys.* 383, 1076–1087, 2002.
- Lattimer, J.M., Prakash, M. Neutron star structure and equation of state. *Astrophys. J.* 550, 426–442, 2001.
- Lattimer, J.M., Pethick, C.J., Prakash, M., et al. Direct URCA process in neutron stars. *Phys. Rev. Lett.* 66, 2701–2704, 1991.
- Lattimer, J.M., Van Riper, K.A., Prakash, M., et al. Rapid cooling and the structure of neutron stars. *Astrophys. J.* 425, 802–813, 1994.
- Lombardo, U., Schulze, H.-J. Superfluidity in neutron star matter, in: Blaschke, D., Glendenning, N., Sedrakian, A. (Eds.), *Physics of Neutron Star Interiors*. Springer, Berlin, pp. 30–53, 2001.
- Lyne, A.G., Pritchard, R.S., Graham-Smith, F., et al. Very low braking index for the Vela pulsar. *Nature* 381, 497–498, 1996.
- Page, D. Thermal evolution of isolated neutron stars, in: Buccheri, R., van Paradijs, J., Alpar, M.A. (Eds.), *The Many Faces of Neutron Stars*. Kluwer, Dordrecht, pp. 539–551, 1998a.
- Page, D. Thermal evolution of isolated neutron stars, in: Shibazaki, N., Kawai, N., Shibata, S., Kifune, T. (Eds.), *Neutron Stars and Pulsars*. Universal Academy Press, Tokyo, pp. 183–194, 1998b.
- Page, D., Applegate, J.H. The cooling of neutron stars by the direct URCA process. *Astrophys. J.* 394, L17–L20, 1992.
- Pavlov, G.G., Teter, M. (private communication) 2002.
- Pavlov, G.G., Zavlin, V.E., Sanwal, D., et al. The X-Ray spectrum of the Vela pulsar resolved with the *Chandra* X-ray observatory. *Astrophys. J.* 552, L129–L133, 2001.
- Pavlov, G.G., Zavlin, V.E., Sanwal, D., et al. 1E 1207.4-5209: the puzzling pulsar at the center of the supernova remnant PKS 1209-51/5. *Astrophys. J.* 569, L95–L98, 2002a.
- Pavlov, G.G., Zavlin, V.E., Sanwal, D. Thermal radiation from neutron stars: *Chandra* results, in: Becker, W., Lesh, H., Trümper, J. (Eds.), 270 WE-Heraeus Seminar on Neutron Stars, Pulsars and Supernova Remnants. MPE, Garching, pp. 273–286, 2002b.
- Pethick, C.J. Cooling of neutron stars. *Rev. Mod. Phys.* 64, 1133–1140, 1992.
- Pons, J.A., Walter, F.M., Lattimer, J.M., et al. Toward a mass and radius determination of the nearby isolated neutron star RX J185635-3754. *Astrophys. J.* 564, 981–1006, 2002.
- Possenti, A., Mereghetti, S., Colpi, M. The pulsed soft X-ray emission from PSR 0656+14. *Astron. Astrophys.* 313, 565–570, 1996.
- Potekhin, A.Y., Yakovlev, D.G. Thermal structure and cooling of neutron stars with magnetized envelopes. *Astron. Astrophys.* 374, 213–226, 2001.
- Potekhin, A.Y., Chabrier, G., Yakovlev, D.G. Internal temperatures and cooling of neutron stars with accreted envelopes. *Astron. Astrophys.* 323, 415–428, 1997.
- Prakash, M., Ainsworth, T.L., Lattimer, J.M. Equation of state and the maximum mass of neutron stars. *Phys. Rev. Lett.* 61, 2518–2521, 1988.
- Rutledge, R.E., Bildsten, L., Brown, E.F., et al. The thermal X-Ray spectra of Centaurus X-4, Aquila X-1, and 4U 1608-522 in quiescence. *Astrophys. J.* 514, 945–951, 1999.
- Rutledge, R.E., Bildsten, L., Brown, E.F., et al. A method for distinguishing between transiently accreting neutron stars and black holes, in quiescence. *Astrophys. J.* 529, 985–996, 2000.
- Rutledge, R.E., Bildsten, L., Brown, E.F., et al. Crustal emission and the quiescent spectrum of the neutron star in KS 1731-260. *Astrophys. J.* 580, 413–422, 2002.
- Slane, P.O., Helfand, D.J., Murray, S.S. New constraints on neutron star cooling from *Chandra* observations of 3C 58. *Astrophys. J.* 571, L45–L49, 2002.
- Tennant, A.F., Becker, W., Juda, M., et al. Discovery of X-ray emission from the Crab pulsar at pulse minimum. *Astrophys. J.* 554, L173–L176, 2001.
- Thorne, K.S. The relativistic equations of stellar structure and evolution. *Astrophys. J.* 212, 825–831, 1977.
- Tsuruta, S., Cameron, A.G.W. Cooling and detectability of neutron stars. *Canad. J. Phys.* 44, 1863–1894, 1966.
- Walter, F.M., Lattimer, J.M. A revised parallax and its implications for RX J185635-3754. *Astrophys. J.* 576, L145–L148, 2002.
- Wijnands, R., Guainazzi, M., van der Klis, M., et al. XMM-Newton observations of the neutron star X-ray transient KS 1731-260 in quiescence. *Astrophys. J.* 573, L45–L49, 2002.
- Winkler, P.F., Tuttle, J.H., Kirshner, R.P., et al. Kinematics of oxygen-rich filaments in Puppis A, in: Roger, R.S., Landecker, T.L. (Eds.), *Supernova Remnants and the Interstellar Medium*. Cambridge University Press, Cambridge, pp. 65–71, 1988.
- Yakovlev, D.G., Haensel, P. What we can learn from observations of cooling neutron stars. *Astron. Astrophys.* 407, 259–264, 2003.
- Yakovlev, D.G., Levenfish, K.P., Shibano, Yu.A. Cooling of neutron stars and superfluidity in their cores. *Physics – Uspekhi* 42, 737–778, 1999.
- Yakovlev, D.G., Kaminker, A.D., Gnedin, O.Y., et al. Neutrino emission from neutron stars. *Phys. Rep.* 354, 1–155, 2001a.
- Yakovlev, D.G., Kaminker, A.D., Gnedin, O.Y. 1S_0 neutron pairing vs. observations of cooling neutron stars. *Astron. Astrophys.* 379, L5–L8, 2001b.
- Yakovlev, D.G., Levenfish, K.P., Haensel, P. Thermal states of transiently accreting neutron stars. *Astron. Astrophys.* 407, 265–271, 2003.
- Yakovlev, D.G., Gnedin, O.Y., Kaminker, A.D., et al. Cooling of superfluid neutron stars, in: Becker, W., Lesh, H., Trümper, J. (Eds.), 270 WE-Heraeus Seminar on Neutron Stars, Pulsars and Supernova Remnants. MPE, Garching, pp. 287–299, 2002a.
- Yakovlev, D.G., Kaminker, A.D., Haensel, P., et al. The cooling neutron star in 3C 58. *Astron. Astrophys.* 389, L24–L27, 2002b.
- Zavlin, V.E., Pavlov, G.G., Trümper, J. The neutron star in the supernova remnant PKS 1209-52. *Astron. Astrophys.* 331, 821–828, 1998.
- Zavlin, V.E., Trümper, J., Pavlov, G.G. X-ray emission from radio-quiet neutron star in Puppis A. *Astrophys. J.* 525, 959–967, 1999.